ground water

Potential Contaminant Pathways from Hydraulically Fractured Shale to Aquifers

by Tom Myers

Abstract

Hydraulic fracturing of deep shale beds to develop natural gas has caused concern regarding the potential for various forms of water pollution. Two potential pathways—advective transport through bulk media and preferential flow through fractures—could allow the transport of contaminants from the fractured shale to aquifers. There is substantial geologic evidence that natural vertical flow drives contaminants, mostly brine, to near the surface from deep evaporite sources. Interpretative modeling shows that advective transport could require up to tens of thousands of years to move contaminants to the surface, but also that fracking the shale could reduce that transport time to tens or hundreds of years. Conductive faults or fracture zones, as found throughout the Marcellus shale region, could reduce the travel time further. Injection of up to 15,000,000 L of fluid into the shale generates high pressure at the well, which decreases with distance from the well and with time after injection as the fluid advects through the shale. The advection displaces native fluids, mostly brine, and fractures the bulk media widening existing fractures. Simulated pressure returns to pre-injection levels in about 300 d. The overall system requires from 3 to 6 years to reach a new equilibrium reflecting the significant changes caused by fracking the shale, which could allow advective transport to aquifers in less than 10 years. The rapid expansion of hydraulic fracturing requires that monitoring systems be employed to track the movement of contaminants and that gas wells have a reasonable offset from faults.

Introduction

The use of natural gas (NG) in the United States has been increasing, with 53% of new electricity generating capacity between 2007 and 2030 projected to be with NG-fired plants (EIA 2009). Unconventional sources account for a significant proportion of the new NG available to the plants. A specific unconventional source has been deep shale-bed NG, including the Marcellus shale primarily in New York, Pennsylvania, Ohio, and West Virginia (Soeder 2010), which has seen over 4000 wells developed between 2009 and 2010 in Pennsylvania (Figure 1). Unconventional shale-bed NG differs from conventional sources in that the host-formation permeability is so low that gas does not naturally flow in timeframes suitable for development. Hydraulic fracturing (fracking, the industry term for the operation; Kramer 2011) loosens the formation to release the gas and provide pathways for it to move to a well.

Fracking injects up to 17 million liters of fluid consisting of water and additives, including benzene at concentrations up to 560 ppm (Jehn 2011), at pressures up to 69,000 kPa (PADEP 2011) into low permeability shale to force open and connect the fractures. This is often done using horizontal drilling through the middle of the shale with wells more than a kilometer long. The amount of injected fluid that returns to the ground surface after fracking ranges from 9% to 34% of the injected fluid (Alleman 2011; NYDEC 2009), although some would be formation water.

Many agency reports and legal citations (DiGiulio et al. 2011; PADEP 2009; ODNR 2008) and peer-reviewed articles (Osborn et al. 2011; White and Mathes

Hydrologic Consultant, 6320 Walnut Creek Road, Reno, NV 89523; (775) 530-1483; fax: (775) 530-1483; tom_myers@charter.net

Received August 2011, accepted February 2012.

doi: 10.1111/j.1745-6584.2012.00933.x

Figure 1. Location of Marcellus shale in the northeastern United States. Location of Marcellus wells (dots) drilled from July 2009 to June 2010 and total Marcellus shale wells in New York and West Virginia. There are 4064 wells shown in Pennsylvania, 48 wells in New York, and 1421 wells in West Virginia. Faulting in the area is documented by PBTGS (2001), Isachsen and McKendree (1977), and WVGES (2011, 2010a, 2010b).

2006) have found more gas in water wells near areas being developed for unconventional NG, documenting the source can be difficult. One reason for the difficulty is the different sources; thermogenic gas is formed by compression and heat at depth and bacteriogenic gas is formed by bacteria breaking down organic material (Schoell 1980). The source can be distinguished based on both C and H isotopes and the ratio of methane to higher chain gases (Osborn and McIntosh 2010; Breen et al. 2007). Thermogenic gas can reach aquifers only by leaking from the well bore or by seeping vertically from the source. In either case, the gas must flow through potentially very thick sequences of sedimentary rock to reach the aquifers. Many studies which have found thermogenic gas in water wells found more gas near fracture zones (DiGiulio et al. 2011; Osborn et al. 2011; Breen et al. 2007), suggesting that fractures are pathways for gas transport.

A pathway for gas would also be a pathway for fluids and contaminants to advect from the fractured shale to the surface, although the transport time would be longer. Fracking fluid has been found in aquifers (DiGiulio et al. 2011; EPA 1987), although the exact source and pathways had not been determined. With the increasing development of unconventional NG sources, the risk to aquifers could be increasing. With so little data concerning the movement of contaminants along pathways from depth, either from wellbores or from deep formations, to aquifers, conceptual analyses are an alternative means to consider the risks.

The intent of this study is to characterize the risk factors associated with vertical contaminant transport from the shale to near-surface aquifers through natural pathways. I consider first the potential pathways for contaminant transport through bedrock and the necessary conditions for such transport to occur. Second, I estimate contaminant travel times through the potential pathways, with a bound on these estimates based on formation hydrologic parameters, using interpretative MODFLOW-2000 (Harbaugh et al. 2000) computations. The modeling does not, and cannot, account for all of the complexities of the geology, which could either increase or decrease the travel times compared to those considered herein. The article also does not include improperly abandoned

boreholes which could cause rapid transport in addition to natural pathways.

Method of Analysis

Using the Marcellus shale region of southern New York (Figure 1), I consider several potential scenarios of transport from shale, 1500 m below ground surface (bgs) to the surface, beginning with pre-development steady state conditions to establish a baseline and then scenarios considering transport after fracking has potentially caused contaminants to reach formations above the shale. To develop the conceptual models and MODFLOW-2000 simulations, it is necessary first to consider the hydrogeology of the shale and the details of hydraulic fracturing, including details of how fracking changes the shale hydrogeologic properties.

Hydrogeology of Marcellus Shale

Shale is a mudstone, a sedimentary rock consisting primarily of clay- and silt-sized particles. It forms through the deposition of fine particles in a low energy environment, such as a lake- or seabed. The Marcellus shale formed in very deep offshore conditions during Devonian time (Harper 1999) where only the finest particles had remained suspended. The depth to the Marcellus shale varies to as much as 3000 m in parts of Pennsylvania, and averages about 1500 m in southern New York (Soeder 2010). Between the shale and the ground surface are layers of sedimentary rock, including sandstone, siltstone, and shale (NYDEC 2009).

Marcellus shale has very low natural intrinsic permeability, on the order of 10^{-16} Darcies (Kwon et al. 2004a, 2004b; Neuzil 1986, 1994). Schulze-Makuch et al. (1999) described Devonian shale of the Appalachian Basin, of which the Marcellus is a major part, as containing "coaly organic material and appear either gray or black" and being "composed mainly of tiny quartz grains <0.005 mm diameter with sheets of thin clay flakes." Median particle size is 0.0069 ± 0.00141 mm with a grain size distribution of <2% sand, 73% silt, and 25% clay. Primary pores are typically 5×10^{-5} mm in diameter, matrix porosity is typically 1% to 4.5% and fracture porosity is typically 7.8% to 9% (Schulze-Makuch et al. 1999 and references therein).

Porous flow in unfractured shale is negligible due to the low bulk media permeability, but at larger scales fractures control and may allow significant flow. The Marcellus shale is fractured by faulting and contains synclines and anticlines that cause tension cracks (Engelder et al. 2009; Nickelsen 1986). It is sufficiently fractured in some places to support water wells just 6 to 10 km from where it is being developed for NG at 2000 m bgs (Loyd and Carswell 1981). Conductivity scale dependency (Schulze-Makuch et al. 1999) may be described as follows:

$$K = Cv^m$$

K is hydraulic conductivity (m/s), C is the intercept of a log-log plot of observed K to scale (the K at a sample volume of 1 m^3), v is sample volume (m^3), and m is a scaling exponent determined with log-log regression; for Devonian shale, C equals $10^{-14.3}$, representing the intercept, and m equals 1.08 (Schulze-Makuch et al. 1999). The very low intercept value is a statistical but not geologic outlier because it corresponds with very low permeability values and demonstrates the importance of fracture flow in the system (Schulze-Makuch et al. 1999). Most of their 89 samples were small because the deep shale is not easily tested at a field-scale and no groundwater models have been calibrated for flow through the Marcellus shale. Considering a 1-km square area with 30-m thickness, the Kh would equal 5.96×10^{-7} m/s (0.0515 m/d). This effective K is low and the shale would be an aquitard, but a leaky one.

Contaminant Pathways from Shale to the Surface

Thermogenic NG found in near-surface water wells (Osborn et al. 2011; Breen et al. 2007) demonstrates the potential for vertical transport of gas from depth. Osborn et al. (2011) found systematic circumstantial evidence for higher methane concentrations in wells within 1 km of Marcellus shale gas wells. Potential pathways include advective transport through sedimentary rock, fractures and faults, and abandoned wells or open boreholes. Gas movement through fractures depends on fracture width (Etiope and Martinelli 2002) and is a primary concern for many projects, including carbon sequestration (Annunziatellis et al. 2008) and NG storage (Breen et al. 2007). Open boreholes and improperly sealed water and gas wells can be highly conductive pathways among aquifers (Lacombe et al. 1995; Silliman and Higgins 1990).

Pathways for gas suggest pathways for fluids and contaminants, if there is a gradient. Vertical hydraulic gradients of a up to a few percent, or about 30 m over 1500 m, exist throughout the Marcellus shale region as may be seen in various geothermal developments in New York (TAL 1981). Brine more than a thousand meters above their evaporite source (Dresel and Rose 2010) is evidence of upward movement from depth to the surface. The Marcellus shale, with salinity as high as 350,000 mg/L (Soeder 2010; NYDEC 2009), may be a primary brine source. Relatively uniform brine concentrations over large areas (Williams et al. 1998) suggest widespread advective transport. The transition from brine to freshwater suggests a long-term equilibrium between the upward movement of brine and downward movement of freshwater. Faults, which occur throughout the Marcellus shale region (Figure 1) (Gold 1999), could provide pathways (Konikow 2011; Caine et al. 1996) for more concentrated advective and dispersive transport. Brine concentrating in faults or anticline zones reflects potential preferential pathways (Wunsch 2011; Dresel and Rose 2010; Williams 2010; Williams et al. 1998).

In addition to the natural gradient, buoyancy would provide an additional initial upward push. At TDS equal to 350,000 mg/L, the density at 25 °C is approximately

1290 kg/m^3, or more than 29% higher than freshwater. The upward force would equal the difference in weight between the injected fluid and displaced brine. As an example, if 10,000,000 L does not return to the surface as flowback (Jehn 2011), the difference in mass between the volume of fracking fluid and displaced brine is approximately 3,000,000 kg, which would cause an initial upward force. The density difference would dissipate as the salt concentration in the fracking fluid increases due to diffusion across the boundary between the fluid and the brine.

In just Pennsylvania, more than 180,000 wells had been drilled prior to any requirement for documenting their location (Davies 2011), therefore the location of many wells is unknown and some have probably been improperly abandoned. These pathways connect aquifers through otherwise continuous aquitards; overpressurization of lower aquifers due to injection near the well pathway could cause rapid transport to higher aquifers (Lacombe et al. 1995). In the short fracking period, the region that is overpressurized remains relatively close to the gas well (see modeling analysis below), therefore it should be possible for the driller to locate nearby abandoned wells that could be affected by fracking. This article does not consider the potential contamination although unlocated abandoned wells of all types must be considered a potential and possibly faster source for contamination due to fracking.

Effect of Hydraulic Fracturing on Shale

Fracking increases the permeability of the targeted shale to make extraction of NG economically efficient (Engelder et al. 2009; Arthur et al. 2008). Fracking creates fracture pathways with up to 9.2 million square meters of surface area in the shale accessible to a horizontal well (King 2010; King et al. 2008) and connects natural fractures (Engelder et al. 2009; King et al. 2008). No post-fracking studies that documented hydrologic properties were found while researching this article (there is a lack of information about pre- and post-fracking properties; Schweitzer and Bilgesu 2009), but it is reasonable to assume the K increases significantly because of the newly created and widened fractures.

Fully developed shale typically has wells spaced at about 300-m intervals (Edwards and Weisset 2011; Soeder 2010). Up to eight wells may be drilled from a single well pad (NYDEC 2009; Arthur et al. 2008), although not in a perfect spoke pattern. Reducing by half the effective spacing did not enhance overall productivity (Edwards and Weisset 2011) which indicates that 300-m spacing creates sufficient overlap among fractured zones to assure adequate gas drainage. The properties controlling groundwater flow would therefore be affected over a large area, not just at a single horizontal well or set of wells emanating from a single well pad.

Fracking is not intended to affect surrounding formations, but shale properties vary over short ranges (King 2010; Boyer et al. 2006) and out-of-formation fracking is not uncommon. In the Marcellus shale, out-of-formation fracks have been documented 500 m above the top of the shale (Fisher and Warpinski 2011). These fractures could contact higher conductivity sandstone, natural fractures, or unplugged abandoned wells above the target shale. Also, fluids could reach surrounding formations just because of the volume injected into the shale, which must displace natural fluid, such as the existing brine in the shale.

Analysis of Potential Transport along Pathways

Fracking could cause contaminants to reach overlying formations either by fracking out of formation, connecting fractures in the shale to overlying bedrock, or by simple displacement of fluids from the shale into the overburden. Advective transport, considered as simple particle velocity, will manifest if there is a significant vertical component to the regional hydraulic gradient.

Numerical modeling, completed with the MODFLOW-2000 code (Harbaugh et al. 2000), provides flexibility to consider potential conceptual flow scenarios, but should be considered interpretative (Hill and Tiedeman 2007). The simulation considers the rate of vertical transport of contaminants to near the surface for the different conceptual models, based on an expected, simplified, realistic range of hydrogeologic aquifer parameters.

MODFLOW-2000 is a versatile numerical modeling code, but there is insufficient data regarding the geology and water chemistry between aquifers and the deep shale, such as salinity profiles or data concerning mixing of the brine with fracking fluid, to best use its capabilities. As more data becomes available, it may be useful to consider simulating the added upward force caused by the brine by using the SEAWAT-2000 module (Langevin et al. 2003).

Vertical flow would be perpendicular to the general tendency for sedimentary layers to have higher horizontal than vertical conductivity. Fractures and improperly abandoned wells would provide pathways for much quicker vertical transport than general advective transport. This article considers the fractures as vertical columns with model cells having much higher conductivity than the surrounding bedrock. The cell discretization is fine, so the simulated width of the fracture zones is realistic. Dual porosity modeling (Shoemaker et al. 2008) is not justified because turbulent vertical flow through the fractures is unlikely, except possibly during the actual fracking that causes out-of-formation fractures, a scenario not simulated here. MODFLOW-2000 has a module, MNW (Halford and Hanson 2002), that could simulate rapid transport through open bore holes. MNW should be used in situations where open boreholes or improperly abandoned wells are known or postulated to exist.

The thickness of the formations and fault would affect the simulation, but much less than the several-order-of-magnitude variation possible in the shale properties. The overburden and shale thickness were set equal to 1500 and 30 m, respectively, similar to that observed in southern New York. The estimated travel times are proportional for thicker or thinner sections. The overburden could be predominantly sandstone, with sections of shale, mudstone, and limestone. The vertical fault is assumed

to be 6-m thick. The fault is an attempt at considering fracture flow, but the simulation treats the 6-m wide fault zone as homogeneous, which could underestimate the real transport rate in fracture-controlled systems which could be highly affected by dispersion. The simulation also ignores diffusion between the fracture and the adjacent shale matrix (Konikow 2011).

There are five conceptual models of flow and transport of natural and post-fracking transport from the level of the Marcellus shale to the near-surface to consider herein:

1. The natural upward advective flow due to a head drop of 30 m from below the Marcellus shale to the ground surface, considering the variability in both shale and overburden K. This is a steady state solution for upward advection through a 30-m thick shale zone and 1500-m overburden. Table 1 shows the chosen K values for shale and sandstone.
2. Same as number 1, but with a vertical fracture connecting the shale with the surface, created using a high-conductivity zone in a row of cells extending through all from above the shale to the surface. This emulates the conceptual model postulated for flow into the alluvial aquifers near stream channels, the location of which may be controlled by faults (Williams et al. 1998). The fault K varies from 10 to 1000 times the surrounding bulk sandstone K (K_{ss}).
3. This scenario tests the effect of extensive fracturing in the Marcellus shale by increasing the shale K (K_{sh}) from 10 to 1000 times its native value over an extensive area. This transient solution starts with initial conditions being a steady state solution from scenario 1. The K_{sh} increases from 10 to 1000 times at the beginning of the simulation, to represent the relatively instantaneous change on the regional shale hydrogeology imposed by the fracking. The simulation estimates both the changes in flux and the time for the system to reach equilibrium.
4. As number 3, considering the effect of the same changes in shale properties but with a fault as in number 2.
5. This scenario simulates the actual injection of 13 to 17 million liters of fluid in 5 d into fractured shale from a horizontal well with and without a fault.

Table 1
Sandstone (ss) and Shale (sh) Conductivity (K) (m/d) and the Steady State Flux (m^3/d) for Model 1 Scenarios

Flux	K_{ss}	K_{sh}
1.7	0.1	0.00001
1.8	0.5	0.00001
1.9	1	0.00001
1.9	5	0.00001
2.0	10	0.00001
2.0	50	0.00001
2.0	100	0.00001
1.7	0.1	0.00001
9.5	0.1	0.00005
19.0	0.1	0.0001
81.2	0.1	0.0005
135.9	0.1	0.001
291.5	0.1	0.005
340.9	0.1	0.01
394.3	0.1	0.05
401.8	0.1	0.1
409.2	0.1	0.5
40.7	0.001	0.1
186.0	0.005	0.1
339.1	0.01	0.1
988.3	0.05	0.1
1297.3	0.1	0.1
1748.0	0.5	0.1
1826.1	1	0.1
1902.8	5	0.1
1915.4	10	0.1
338.3	0.1	0.01
984.1	0.5	0.01
1292.5	1	0.01
1731.5	5	0.01
1816.0	10	0.01
17.4	1	0.0001
86.3	1	0.0005
176.7	1	0.001
775.1	1	0.005
1292.5	1	0.01
2746.8	1	0.05
3183.2	1	0.1
3650.5	1	0.5
3719.9	1	1

Model Setup

The model domain was 150 rows and columns spaced at 3 m to form a 450-m square (Figure 2) with 50 layers bounded with no flow boundaries. The 30-m thick shale was divided into 10 equal thickness layers from layer 40 to 49. The overburden layer thickness varied from 3 m just above the shale to layer 34, 6 m from layer 33 to 29, 9 m from layer 28 to 26, 18 m in layer 25, 30 m from layer 24 to 17, 60 m from layer 16 to 6, 90 m from layer 5 to 3, and 100 m in layers 2 and 1. A 6-m wide column from layer 39 to the surface is added for some scenarios in the center two rows to simulate a higher K fault.

The model simulated vertical flow between constant head boundaries in layers 50 and 1, as a source and sink, so that the overburden and shale properties control the flow. The head in layers 50 and 1 was 1580 and 1550 m, respectively, to create a gradient of 0.019 over the profile. Varying the gradient would have much less effect on transport than changing K over several orders of magnitude and was therefore not done.

Scenario 5 simulates injection using a WELL boundary in layer 44, essentially the middle of the shale, from columns 25 to 125 (Figure 2). It injects 15 million liters over one 5-d stress period, or 3030 m^3/d into 101 model cells at the WELL. The modeled K_{sh} was changed to its

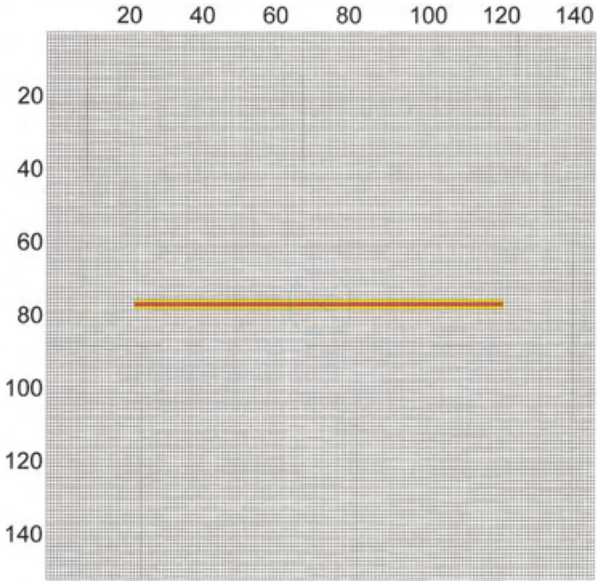

Figure 2. Model grid through layer 44 showing the horizontal injection WELL (red) and DRAIN cells (yellow) used to simulate flowback. There is only one monitoring well because the off-center well is not used in layer 44.

assumed fracked value at the beginning of the simulation. Simulating high rate injection generates very high heads in the model domain, similar to that found simulating oil discharging from the well in the Deepwater Horizon crisis (Hsieh 2011) and water quality changes caused by underground coal gasification (Contractor and El-Didy 1989). DRAIN boundaries on both sides of the WELL simulated return flow for 60 d after the completion of (Figure 2), after which the DRAIN was deactivated. The 60 d were broken into four stress periods, 1, 3, 6, and 50 d long, to simulate the changing heads and flow rates. DRAIN conductance was calibrated so that 20% of the injected volume returned within 60 d to emulate standard industry practice (Alleman 2011; NYDEC 2009). Recovery, continuing relaxation of the head at the well and the adjustment of the head distribution around the domain, occurred during the sixth period which lasted for 36,500 d.

There is no literature guidance to a preferred value for fractured shale storage coefficient, so I estimated S with a sensitivity analysis using scenario 3. With fractured K_{sh} equal to 0.001 m/d, two orders of magnitude higher than the in situ value, the time to equilibrium resulting from simulation tests of three fractured shale storage coefficients, 10^{-3}, 10^{-5}, and 10^{-7}/m, varied twofold (Figure 3). The slowest time to equilibrium was for $S = 10^{-3}$/m (Figure 3), which was chosen for the transient simulations because more water would be stored in the shale and flow above the shale would change the least.

Results

Scenario 1

Table 1 shows the conductivity and flux values for various scenarios. The steady state travel time

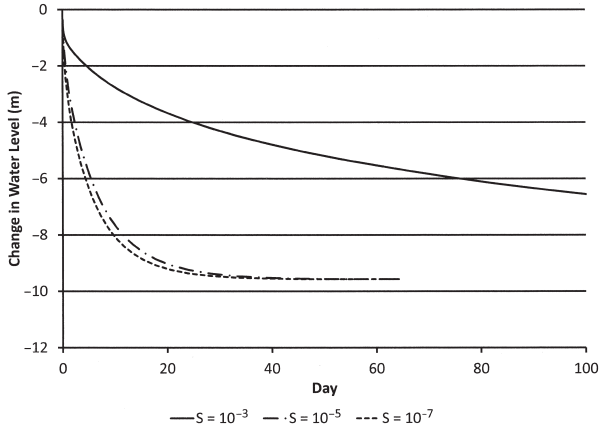

Figure 3. Sensitivity of the modeled head response to the storage coefficient used in the fractured shale for model layer 39 just above the shale.

for a particle through 1500 m of sandstone and shale equilibrates with one of the formations controlling the advection (Figure 4). For example, when the K_{sh} equals 1×10^{-5} m/d, transport time does not vary with K_{ss}. For K_{ss} at 0.1 m/d, transport time for varying K_{sh} ranges from 40,000 to 160 years. The lower travel time estimate is for K_{sh} similar to that found by Schulze-Makuch et al. (1999). The shortest simulated transport time of about 20 years results from both the sandstone and shale K equaling 1 m/d. Other sensitivity scenarios emphasize the control exhibited by one of the media (Figure 4). If K_{sh} is low, travel time is very long and not sensitive to K_{ss}.

Scenario 2

The addition of a fault with K one to two orders of magnitude more conductive than the surrounding sandstone increased the particle travel rate by about 10 times (compare Figure 5 with Figure 4). The fault K controlled the transport rate for K_{sh} less than 0.01 m/d. A highly

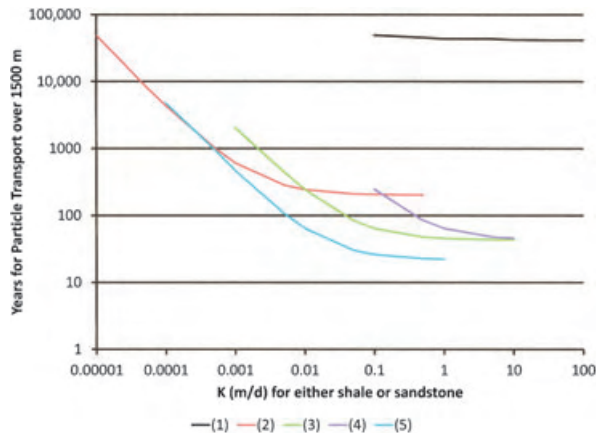

Figure 4. Sensitivity of particle transport time over 1500 m for varying shale and sandstone vertical K. Effective porosity equals 0.1. (1)—varying K_{ss}, $K_{sh} = 10^{-5}$ m/d; (2)—varying K_{ss}, $K_{sh} = 0.1$ m/d; (3)—varying K_{ss}, $K_{sh} = 0.1$ m/d; (4)—varying K_{ss}, $K_{sh} = 0.01$ m/d; and (5)—varying K_{ss}, $K_{sh} = 1.0$ m/d.

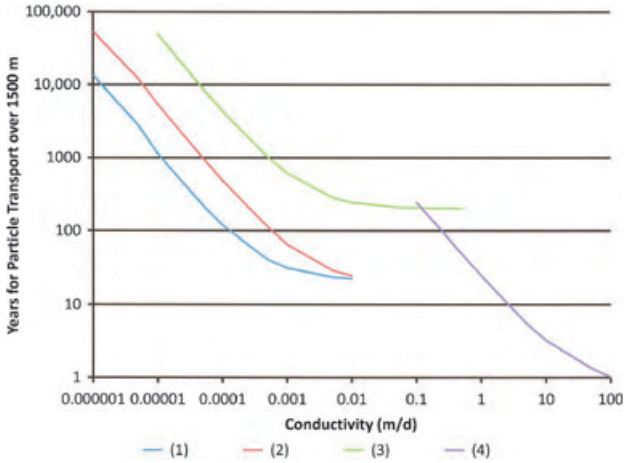

Figure 5. Variability of transport through various scenarios of changing the K for the fault or shale. Effective porosity equals 0.1. (1)—varying K_{sh}, $K_{sh} = 0.01$ m/d; (2)—varying K_{sh}, $K_{sh} = 0.1$ m/d; (3)—no fault; (4)—varying K fault, $K_{sh} = 0.1$ m/d, $K_{sh} = 0.01$ m/d. Unless specified, the vertical fault has $K = 1$ m/d for variable K_{sh}.

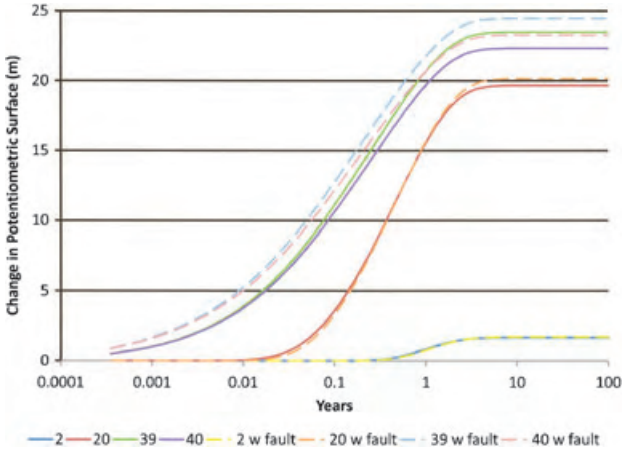

Figure 6. Monitoring well water levels for specified model layers due to fracking of the shale; monitor well in the center of the domain, including in the fault, K of the shale changes from 0.00001 to 0.01 m/d at the beginning of the simulation.

conductive fault could transport fluids to the surface in as little as a year for K_{sh} equal to 0.01 m/d (Figure 5). However, a fault did not significantly change the overall model flux, so with fault values are not shown in Table 1.

Scenarios 3 and 4

Scenarios 3 and 4 estimate the time to establish a new equilibrium once the K_{sh} changes, due to fracking, between values specified in scenarios 1 and 2. Equilibrium times vary by model layer as the changes propagate through the domain, and flux rate for the simulated changes imposed on natural background conditions. The fracking-induced changes cause a significant decrease in the head drop across the shale and the time for adjustment of the potentiometric surface to a new steady state depends on the new shale properties.

The time to equilibrium for one scenario 3 simulation, K_{sh} changing from 10^{-5} to 10^{-2} m/d with K_{ss} equal to 0.1 m/d, varied from 5.5 to 6.5 years, depending on model layer (Figure 6). Near the shale (layers 39 and 40), the potentiometric surface increased from 23 to 25 m reflecting the decreased head drop across the shale. One hundred meters higher, in layer 20, the potentiometric surface increased about 20 m. Simulation of scenario 4, with a fault with $K = 1$ m/d, decreased the time to equilibrium to from 3 to 6 years within the fault zone, depending on model layer (Figure 6). Highly fractured sandstone would allow more vertical transport, but advective flow would also increase so that the base K_{ss} would control the overall rate.

The flux across the upper boundary changed within 100 years for scenario 3 from 1.7 to 345 m^3/d, or 0.000008 to 0.0017 m/d, reflecting control by K_{ss}. There is little difference in the equilibrium fluxes between scenario 3 and 4 indicating that the fault primarily affects the time to equilibrium rather than the long-term flow rate.

Scenario 5: Simulation of Injection

The injection scenarios simulate 15 million liters entering the domain at the horizontal well and the subsequent potentiometric surface and flux changes throughout. The highest potentiometric surface increases (highest injection pressure) occurred at the end of injection (Figure 7), with a 2400 m increase at the horizontal well. The simulated peak pressure both decreased and occurred longer after the cessation of injection with distance from the well (Figures 7 and 8). The pressure at the well returned to within 4 m of pre-injection levels in about 300 d (Figure 7). After injection ceases, the peak pressure simulated further from the well occurs longer from the time of cessation, which indicates there is a pressure divide beyond which fluid continues to flow away from the well bore while within which the fluid flows toward the well bore. The simulated head returned to near pre-injection levels slower with distance from the well (Figure 7), with levels at the edge of the shale (layer 40) and in the near-shale sandstone (layer 39) requiring several hundred days to recover. After recovering from injection, the potentiometric surface above the shale increased in response to flux through the shale adjusting to the change in shale properties (Figure 8), as simulated in scenario 3. The scenario required about 6000 d (16 years) for the potentiometric surface to stabilize at new, higher, levels (Figure 8). Removing the fault from the simulation had little effect on the time to stabilization, and is not shown.

Prior to injection, the steady flux for in situ shale ($K_{sh} = 10^{-5}$ m/d) was generally less than 2 m^3/d and varied little with K_{ss} (Figure 4). Once the shale was fractured, the sandstone controlled the flux which ranges from 38 to 135 m^3/d as K_{ss} ranges from 0.01 to 0.1 m/d (Figure 9), resulting in particle travel times of 2390 and 616 years, respectively. More conductive shale would allow faster transport (Figure 4). Adding a fault to the scenario with K_{ss} equal to 0.01 m/d increased the flux to approximately 63 m^3/d and decreased the particle travel

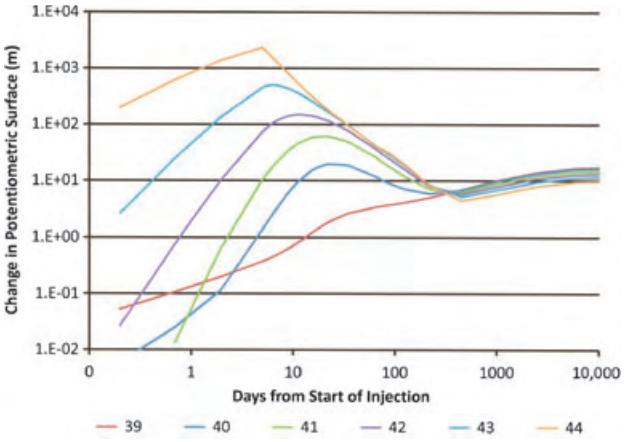

Figure 7. Simulated potentiometric surface changes by layer for specified injection and media properties. The monitoring point is in the center of the domain. Fault is included. K_{sh} = 0.01 m/d, K_{sh} = 0.001 m/d. S (fractured shale) = 0.001/m, S (ss) = 0.0001/m.

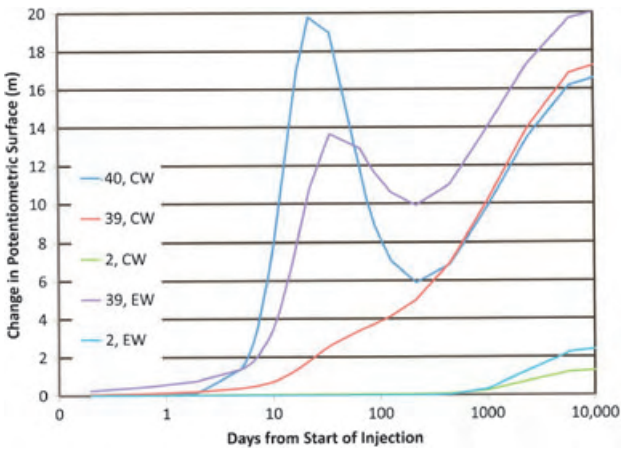

Figure 8. Simulated potentiometric surface changes for layers within the shale and sandstone. CW is center monitoring well and EW is east monitoring well, about 120 m from the centerline. Fault is included. The line for layer 2, CW plots beneath the line for layer 2, EW. K_{ss} = 0.01 m/d, K_{sh} = 0.001 m/d, S (fractured shale) = 0.001/m, S (ss) = 0.0001/m.

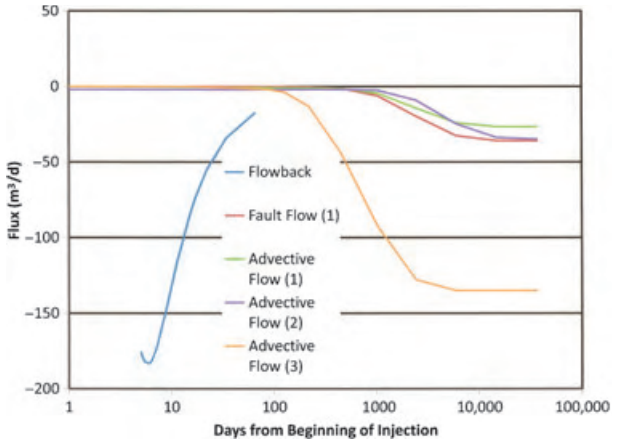

Figure 9. Comparison of flux for three scenarios. Flowback is the same for all scenarios. (1): Kss = 0.01 m/d, Ksh = 0.001 m/d, Fault K = 1 m/d; (2): Kss = 0.01 m/d, Ksh = 0.001 m/d, no fault; (3) Kss = 0.1 m/d, Ksh = 0.001 m/d, no fault.

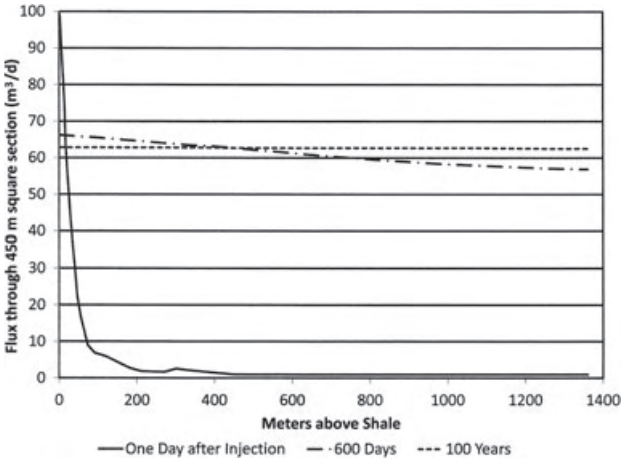

Figure 10. Upward flux across the domain section as a function of distance above the top of the shale layer. Cross section is 202,500 m^2.

time to 31 years. Approximately, 36 m^3/d flowed through the fault (Figure 9). The fault properties control the particle travel time, especially if the fault K is two or more orders of magnitude higher than the sandstone.

Simulated flowback varied little with K_{sh} because it had been calibrated to be 20% of the injection volume. A lower storage coefficient or higher K would allow the injected fluid to move further from the well, which would lead to less flowback.

Vertical flux through the overall section with a fault varies significantly with time, due to the adjustments in potentiometric surface. One day after injection, vertical flux exceeds significantly the pre-injection flux about 200 m above the shale (Figure 10). After 600 d, the vertical flux near the shale is about 68 m^3/d and in layer 2 about 58 m^3/d; it approaches steady state through all sections after 100 years with flux equaling about 62.6 m^3/d. The 100-year flux is 61.5 m^3/d higher than the pre-injection flux because of the changed shale properties.

Discussion

The interpretative modeling completed herein has revealed several facts about fracking. First, MODFLOW can be coded to adequately simulate fracking. Simulated pressures are high, but velocities even near the well do not violate the assumptions for Darcian flow. Second, injection for 5 d causes extremely high pressure within the shale. The pressure decreases with distance from the well. The time to maximum pressure away from the well lags the time of maximum pressure at the well. The pressure drops back to close to its pre-injection level

at the well within 300 d, indicating the injection affects the flow for significantly longer periods than just during the fracking operation. Although the times may vary based on media properties, the difference would be at most a month or so, based on the various combinations of properties simulated. The system transitions within 6 years due to changes in the shale properties. The equilibrium transport rate would transition from a system requiring thousands of years to one requiring less than 100 years within less than 10 years.

Third, most of the injected water in the simulation flows vertically rather than horizontally through the shale. This reflects the higher K_{ss} 20 m above the well and the no flow boundary within 225 m laterally from the well, which emulates in situ shale properties that would manifest at some distance in the shale.

Fourth, the interpretative model accurately and realistically simulates long-term steady state flow conditions, with an upward flow that would advect whatever conservative constituents exist at depth. Using low, unfractured K values, the transport simulation may correspond with advective transport over geologic time although there are conditions for which it would occur much more quickly (Figure 4). If the K_{sh} is 0.01 m/d, transport could occur on the order of a few hundreds of years. Faults through the overburden could speed the transport time considerably. Reasonable scenarios presented herein suggest the travel time could be decreased further by an order of magnitude.

Fifth, fracking increases the K_{sh} by several orders of magnitude. Out-of-formation fracking (Fisher and Warpinski 2011) would increase the K in the overburden, thereby changing the regional hydrogeology. Vertical flow could change over broad areas if the expected density of wells in the Marcellus shale region (NYDEC 2009) actually occurs.

Sixth, if newly fractured shale or out-of-formation fractures come close to contacting fault fracture zones, contaminants could reach surface areas in tens of years, or less. Faults can decrease the simulated particle travel time several orders of magnitude.

Conclusion

Fracking can release fluids and contaminants from the shale either by changing the shale and overburden hydrogeology or simply by the injected fluid forcing other fluids out of the shale. The complexities of contaminant transport from hydraulically fractured shale to near-surface aquifers render estimates uncertain, but a range of interpretative simulations suggest that transport times could be decreased from geologic time scales to as few as tens of years. Preferential flow through natural fractures fracking-induced fractures could further decrease the travel times to as little as just a few years.

There is no data to verify either the pre- or post-fracking properties of the shale. The evidence for potential vertical contaminant flow is strong, but there are also almost no monitoring systems that would detect contaminant transport as considered herein. Several improvements could be made.

- Prior to hydraulic fracturing operations, the subsurface should be mapped for the presence of faults and measurement of their properties.
- A reasonable setback distance from the fracking to the faults should be established. The setback distance should be based on a reasonable risk analysis of fracking increasing the pressures within the fault.
- The properties of the shale should be verified, post-fracking, to assess how the hydrogeology will change.
- A system of deep and shallow monitoring wells and piezometers should be established in areas expecting significant development, before that development begins (Williams 2010).

Acknowledgments

This research was funded by the Park Foundation and Catskill Mountainkeepers. The author thanks Anthony Ingraffea, Paul Rubin, Evan Hansen, two anonymous reviews, and the journal editor for helpful comments on this article.

References

Alleman, D. 2011. Water used for hydraulic fracturing: Amounts, sources, reuse, and disposal. In *Hydraulic Fracturing of the Marcellus Shale*, National Ground Water Association short course. Baltimore, Maryland.

Annunziatellis, A., S.E. Beaubien, S. Bigi, G. Ciotoli, M. Coltella, and S. Lombardi. 2008. Gas migration along fault systems and through the vadose zone in the Latera calder (central Italy): Implications for CO_2 geological storage. *International Journal of Greenhouse Gas Control* 2; 353–372. DOI: 10.1016/j.ijggc.2008.02.003.

Arthur, J.D., B. Bohm, and M. Layne. 2008. *Hydraulic Fracturing Consideration for Natural Gas Wells of the Marcellus Shale.* Cincinnati, Ohio: Ground Water Protection Council.

Boyer, C., J. Kieschnick, R. Suarez-Rivera, R.E. Lewis, and G. Waters. 2006. Producing gas from its source. *Oilfields Review* 18, no. 3: 36–49.

Breen, K.J., K. Revesz, F.J. Baldassare, and S.D. McAuley. 2007. Natural gases in ground water near Tioga Junction, Tioga County, north-central Pennsylvania—Occurrence and use of isotopes to determine origins. Scientific Investigations Report Series 2007-5085. Reston, Virginia: U.S. Geological Survey.

Caine, J.S., J.P. Evans, and C.B. Forster. 1996. Fault zone architecture and permeability structure. *Geology* 24, no. 11: 1025–1028.

Contractor, D.N., and S.M.A. El-Didy. 1989. Field application of a finite-element water-quality model to a coal seam with UCG burns. *Journal of Hydrology* 109: 57–64.

Davies, R.J. 2011. Methane contamination of drinking water caused by hydraulic fracturing remains unproven. *Proceedings of the National Academy of Sciences USA* 108: E871.

DiGiulio, D.C., R.T. Wilkin, C. Miller, and G. Oberly. 2011. *DRAFT: Investigation of Ground Water Contamination near Pavillion, Wyoming.* Ada, Oklahoma: U.S. Environmental Protection Agency, Office of Research and Development.

Dresel, P.E., and A.W. Rose. 2010. Chemistry and origin of oil and gas well brines in western Pennsylvania. 4th ser., Open-File Report OFOG 10–01.0, 48. Harrisburg: Pennsylvania Geological Survey.

Edward, K.L., and S. Weisset. 2011. Marcellus shale hydraulic fracturing and optimal well spacing to maximize recovery and control costs. Paper 140463 in *SPE Hydraulic Fracturing Technology Conference*, January 24–26, 2011, The Woodlands, Texas.

Energy Information Administration (EIA). 2009. *Annual Energy Outlook with Projections to 2030.* Washington, D.C.: U.S. Department of Energy. http://www.eia.doe.gov/oiaf/aeo/ (accessed May 23, 2011).

Engelder, T., G.G. Lash, and R.S. Uzcategui. 2009. Joint sets that enhance production from Middle and Upper Devonian gas shales of the Appalachian Basin. *AAPG Bulletin* 93, no. 7: 857–889.

Environmental Protection Agency (EPA). 1987. Report to congress, management of wastes from the exploration, development, and production of crude oil, natural gas, and geothermal energy, volume 1 of 3, oil and gas. Washington, DC: EPA.

Etiope, G., and G. Martinelli. 2002. Migration of carrier and trace gases in the geosphere: an overview. *Physics of the Earth and Planetary Interiors* 129: 3–4.

Fisher, K., and N. Warpinski. 2011. Hydraulic fracture-height growth: real data. Paper SPE 145949 presented at the Annual Technical Conference and Exhibition, Denver, Colorado. DOI: 10.2118/145949-MS.

Gold, D. 1999. Lineaments and their interregional relationships. In *The Geology of Pennsylvania*, ed. C.H. Schultz, 307–313. Harrisburg: Pennsylvania Department of Conservation and Natural Resources.

Halford, K.J., and R.T. Hanson. 2002. User guide for the drawdown-limited, multi-node well (MNW) package for the U.S. Geological Survey's modular three-dimensional finite-difference ground-water flow model, Versions MODFLOW-96 and MODFLOW-2000, 33. Open-File Report 02-293. Sacramento, California: U.S. Geological Survey.

Harbaugh, A.W., E.R. Banta, M.C. Hill, and M.G. McDonald. 2000. Modflow-2000, the U.S. Geological Survey modular ground-water model—User guide to modularization, concepts and the ground-water flow process. Open-File Report 00-92. Reston, Virginia: U.S. Geological Survey.

Harper, J.A. 1999. Devonian. In *The Geology of Pennsylvania*, ed. C.H. Schultz, 108–127. Harrisburg: Pennsylvania Department of Conservation and Natural Resources.

Hill, M.C., and C.R. Tiedeman. 2007. *Effective Groundwater Model Calibration: With Analysis of Data, Sensitivities, Predictions, and Uncertainty.* Hoboken, New Jersey: John Wiley and Sons.

Hsieh, P.A. 2011. Application of MODFLOW for oil reservoir simulation during the Deepwater Horizon crisis. *Ground Water* 49, no. 3: 319–323. DOI: 10.1111/j.1745-6584.2011.00813.x.

Isachsen, Y.W., and W. McKendree. 1977. *Preliminary Brittle Structure Map of New York, Map and Chart Series No. 31.* Albany, New York: New York State Museum.

Jehn, P. 2011. Well and water testing—What to look for and when to look for it. In *Groundwater and Hydraulic Fracturing of the Marcellus Shale*, National Gound Water Association short course. Baltimore, Maryland.

King, G. 2010. Thirty years of gas shale fracturing: What have we learned? Paper SPE 133456 presented at the *SPE Annual Technical Conference and Exhibition*, September 19–22, 2010, Florence, Italy.

King, G.E., L. Haile, J. Shuss, and T.A. Dobkins. 2008. Increasing fracture path complexity and controlling downward fracture growth in the Barnett shale. Paper 119896 presented at the *SPE Shale Gas Production Conference*, November 16–18, 2008, Fort Worth, Texas.

Konikow, L.F. 2011. The secret to successful solute-transport modeling. *Ground Water* 49, no. 2: 144–159. DOI: 10.1111/j.1745-6584.2010.00764x.

Kramer, D. 2011. Shale-gas extraction faces growing public and regulatory challenges. *Physics Today* 64, no. 7: 23–25.

Kwon, O., A.K. Kronenberg, A.F. Gangi, B. Johnson, and B.E. Herbert. 2004a. Permeability of illite-bearing shale: 1. Anisotropy and effects of clay content and loading. *Journal of Geophysical Research* 109: B10205. DOI: 10.1029/2004/JB003052.

Kwon, O., B.E. Herbert, and A.K. Kronenberg. 2004b. Permeability of illite-bearing shale: 2. Influence of fluid chemistry on flow and functionally connected pores. *Journal of Geophysical Research* 109: B10206. DOI:10.1029/2004JB00 3055.

Lacombe, S., E.A. Sudickey, S.K. Frape, and A.J.A. Unger. 1995. Influence of leak boreholes on cross-formational groundwater flow and contaminant transport. *Water Resources Research* 31, no. 8: 1871–1882.

Langevin, C.D., W.B. Shoemaker, and W. Guo. 2003. MODF LOW-2000, the U.S. Geological Survey modular groundwater model–Documentation of the SEAWAT-2000 version with the variable-density flow process (VDF) and the integrated MT3DMS transport process (IMT), 43 p. Open-File Report 03-426. Tallahassee, Florida: U.S. Geological Survey.

Loyd, O.B., and L.D. Carswell. 1981. Groundwater resources of the Williamsport region, Lycoming County, Pennsylvania. Water Resources Report 51. Pennsylvania: Department of Environmental Resources.

Neuzil, C.E. 1994. How permeable are clays and shales? *Water Resources Research* 30, no. 2: 145–150.

Neuzil, C.E. 1986. Groundwater flow in low-permeability environments. *Water Resources Research* 22, no. 8: 1163–1195.

New York State Department of Environmental Conservation (NYDEC). 2009. *Draft Supplemental Generic Environmental Impact Statement on the Oil, Gas and Solution Mining Regulatory Program—Well Permit Issuance for Horizontal Drilling and High-Volume Hydraulic Fracturing to Develop the Marcellus Shale and Other Low-Permeability Gas Reservoirs.* Albany, New York: State Department of Environmental Conservation.

Nickelsen, R.P. 1986. Cleavage duplexes in the Marcellus Shale of the Appalachian foreland. *Journal of Structural Geology* 8, no. 3/4: 361–371.

Ohio Department of Natural Resources (ODNR). 2008. Report on the Investigation of the Natural Gas Invasion of Aquifers in Bainbridge Township of Geauga County, Ohio. ODNR, Division of Mineral Resources Management.

Osborn, S.G., A. Vengosh, N.R. Warner, and R.B. Jackson. 2011. Methane contamination of drinking water accompanying gas-well drilling and hydraulic fracturing. *Proceedings of the National Academy of Sciences* 108, no. 20: 8172–8176.

Osborn, S.G., and J.C. McIntosh. 2010. Chemical and isotopic tracers of the contribution of microbial gas in Devonian organic-rich shales and reservoir sandstones, northern Appalachian Basin. *Applied Geochemistry* 25, no. 3: 456–471.

Pennsylvania Bureau of Topographic and Geologic Survey (PBTGS). 2001. *Bedrock Geology of Pennsylvania (Digital Files).* Harrisburg, Pennsylvania: PA Department of Conservation and Natural Resources.

Pennsylvania Department of Environmental Protection (PADEP). 2011. Marcellus Shale. http://www.dep.state.pa.us/dep/deputate/minres/oilgas/new_forms/marcellus/marcellus.htm (accessed June 1, 2011).

Pennsylvania Department of Environmental Protection (PADEP). 2009. Notice of Violation, Re: Gas Migration Investigation, Dimock Township, Susquehanna County, Letter from S. C. Lobins, Regional Manager, Oil and Gas Management, to Mr. Thomas Liberatore, Cabot Oil and Gas Corporation. February 27, 2009. 4 pp., PADEP, Meadville, Pennsylvania.

Schoell, M. 1980. The hydrogen and carbon isotopic composition of methane from natural gases of various origins. *Geochemica et Cosmochiica Act* 44, no. 5: 649–661.

Schulze-Makuch, D., D.A. Carlson, D.S. Cherkauer, and P. Malik. 1999. Scale dependence of hydraulic conductivity in heterogeneous media. *Ground Water* 37, no. 6: 904–919.

Schweitzer, R., and H.I. Bilgesu. 2009. The role of economics on well and fracture design completions of Marcellus Shale wells. Paper 125975 in SPE *Eastern Regional Meeting*, September 23–25, 2009, Charleston, West Virginia.

Shoemaker, W.B., E.L. Kuniansky, S. Birk, S. Bauer, and E.D. Swain. 2008. Documentation of a conduit flow process (CFP) for MODFLOW-2005. U.S. Geological Survey techniques and methods, Book 6, chapter A24, 50 p. Reston, Virgina: U.S. Geological Survey.

Silliman, S., and D. Higgins. 1990. An analytical solution for steady-state flow between aquifers through an open well. *Ground Water* 28, no. 2: 184–190.

Soeder, D.J. 2010. The Marcellus shale: Resources and reservations. *EOS* 91, no. 32: 277–278.

T.A.L. Research and Development (TAL). 1981. Geology, drill holes, and geothermal energy potential of the basal Cambrian rock units of the Appalachian Basin of New York State. In *Prepared for New York State Energy Research and Development Authority*, 54 p.

West Virginia Geological and Economic Survey (WVGES). 2011. *Completed Wells—Marcellus Shale, West Virginia.* Morgantown, West Virginia: WVGES.

West Virginia Geological and Economic Survey (WVGES). 2010a. *Structural Geologic Map (Faults)—Topo of the Onondaga Limestone or Equivalent, West Virginia.* Morgantown, West Virginia: WVGES.

West Virginia Geological and Economic Survey (WVGES). 2010b. *Structural Geologic Map (Folds)—Topo of the Onondaga Limestone or Equivalent, West Virginia.* Morgantown, West Virginia: WVGES.

White, J.S., and M.V. Mathes. 2006. Dissolved-gas concentration in ground water in West Virginia, 8. Data Series 156. Reston, Virginia: U.S. Geological Survey.

Williams, J.H. 2010. Evaluation of well logs for determining the presence of freshwater, saltwater, and gas above the Marcellus shale in Chemung, Tioga, and Broome Counties, New York. Scientific Investigations Report 2010–5224, 27. Reston, Virginia: U.S. Geological Survey.

Williams, J.H., L.E. Taylor, and D.J. Low. 1998. Hydrogeology and groundwater quality of the Glaciated Valleys of Bradford, Tioga, and Potter Counties, Pennsylvania. Water Resource Report 68. Pennsylvania Dept of Conservation and Natural Resources and U.S. Geological Survey.

Wunsch, D. 2011. Hydrogeology and hydrogeochemistry of aquifers overlying the Marcellus shale. In *Groundwater and Hydraulic Fracturing of the Marcellus Shale*, National Ground Water Association short course. Baltimore, Maryland.